Simplified Analytical Calculation of PM Machines Magnetic Flux Leakage Factor

K. Hruska, P. Dvorak

2022 International Conference on Electrical Machines (ICEM) | 978-1-6654-1432-6/22/$31.00 ©2022 IEEE | DOI: 10.1109/ICEM51905.2022.9910678

***Abstract* -- The permanent magnets used for generation of magnetic field in permanent magnet machines are placed in more or less magnetically conducting environment – electrical steel and air. This causes leakage of the magnetic flux from its desired path through the air gap. This paper describes simplified analytical calculation of magnetic properties of five most commonly used placements of permanent magnets and compares obtained leakage factors. A verification of the results via finite element method is also included.**

***Index Terms*--Electromagnetic modelling, Finite element analysis, Magnetic flux leakage, Permanent magnets**

I. NOMENCLATURE

A	magnetic vector potential
b_b	magnetic bridge width
b_o	slot opening width
B_{last}	last defined magnetic flux density of used steel
B_r	remanent magnetic flux density
B_δ	air gap magnetic flux density
B_σ	leakage path magnetic flux density
d	direct axis
F_{PM}	permanent magnet magnetomotive force
h_b	magnetic bridge height
k_C	Carter's factor
k_δ	air gap length factor
k_σ	permanent magnet leakage flux factor
h_{PM}	permanent magnet height
H_c	coercive magnetic field strength
H_{last}	last defined magnetic field strength of steel
H_δ	air gap magnetic field strength
H_σ	leakage path magnetic field strength
l	iron stack length
l_σ	leakage path length
q	quadrature axis
r_σ	radius of leakage path
R_{PM}	permanent magnet reluctance
R_δ	air gap reluctance
R_σ	leakage path reluctance
S_δ	area of one pole pitch in the air gap
t_p	pole pitch
t_s	stator slot pitch
α_{PM}	mechanical permanent magnet coverage factor
α_δ	electromagnetic pole coverage factor
δ	mechanical air gap length
δ'	electromagnetic air gap length
δ_{max}	maximal air gap above permanent magnets
ΔF	magnetomotive force drop
φ_{PM}	angle between permanent magnets
Φ_{PM}	magnetic flux of permanent magnets
Φ_δ	air gap magnetic flux
Φ_σ	leakage magnetic flux
μ_0	permeability of vacuum
μ_{sat}	permeability of saturated steel
μ_{rPM}	permanent magnet relative permeability
μ_{rsat}	relative permeability of saturated steel

This research has been supported by the Ministry of Education, Youth and Sports of the Czech Republic under the project OP VVV Electrical Engineering Technologies with High-Level of Embedded Intelligence CZ.02.1.01/0.0/0.0/18_069/0009855 and UWB project SGS-2021-021.

K. Hruska is with the Department of Power Electronics and Machines, Faculty of Electrical Engineering, University of West Bohemia, Univerzitni 8, Pilsen, Czech Republic (e-mail: khruska@fel.zcu.cz).

P. Dvorak is with Skoda Electric, a. s., Prumyslova 610/2a, Pilsen, Czech Republic (e-mail: pavel.dvorak@skoda.cz).

II. INTRODUCTION

THE precise design of permanent magnets and permanent magnet electric machines must consider possibly most effects appearing in the electric machine. This includes – among consideration of real properties of the whole magnetic circuit – also properties of the neighbourhood of the permanent magnets. It creates alternative paths to the main magnetic flux, which should go from the rotor to the stator and vice versa. These paths then lead parts of the magnetic flux, which do not assist in creation of the torque of the machine. These parts of the magnetic flux are then commonly denoted as leakage magnetic flux.

The problem of permanent magnet leakage fluxes is in the literature mentioned relatively rarely, whereas most relevant information is to be found in papers and articles. The authors often focus to one single placement of permanent magnets and study their magnetic flux leakage on order to optimize the machine design. The presented solutions are supported most often by finite element method analyses [1], [2], but analytic solutions are also presented [3], [4]. The presented papers cover traditional radial permanent magnet synchronous machines with radial or V-shaped permanent magnets [1], [2], [3], but also axial machines are often in focus of the research [4], [5] as well as transverse flux permanent magnet machines [6], [7]. As an addition to previously mentioned publication [8] adds also a calculation of leakage magnetic flux in axial area of permanent magnets.

Among traditional concepts of electric machines – or magnetic devices – the magnetic flux leakage factor is also being referred in case of non-standard rotor topologies [9] or magnetic retarders [10]. An interesting usage of leakage magnetic flux is presented in [11], where the authors use variations of leakage magnetic flux for controlling characteristics of an interior permanent magnet machine.

In above mentioned works the authors focus on problems

of a single rotor topology, which is being analysed and evaluated without any relation to other permanent magnet placement possibilities. This article offers a unified approach for multiple topologies, which are analytically analysed and compared. For this purpose five most common permanent magnet layouts are chosen and analysed with focus to obtain a simple analytical expression of the permanent magnet leakage flux factor.

III. Analytical Calculation of Permanent Magnet Leakage Flux Factor

For comparison of their physical properties five topologies shown in Fig. 1 were chosen. They include permanent magnets placed on the surface of the rotor (layout "S"), bread-shaped permanent magnets (layout "B"), V-shaped permanent magnets layout (layout "V"), tangentially buried permanent magnets (layout "T") and permanent magnets on the surface of the rotor equipped with pole-shoe (layout "P"). All presented designs were prepared as alternative rotor topologies for a single permanent magnet traction machine, so they were designed to have possibly closest properties, especially regarding peak air gap magnetic flux density.

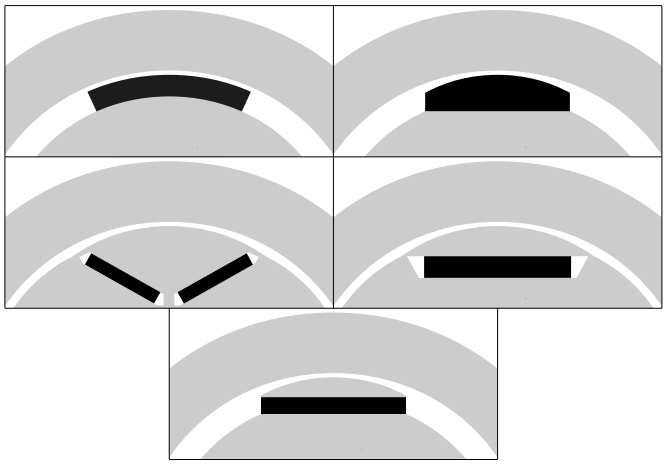

Fig. 1. Schematic visualizations of analysed rotor permanent magnet layouts – "S", "B", "V", "T" and "P" (from left to right).

A. Presumptions of the Analytic Calculations

To obtain a generally valid approach for possibly most permanent magnet rotor layouts, the following presumptions will be considered:

- The permeability of non-saturated iron is considered to be infinite, $\mu_{Fe} \to \infty$.
- The permeability of saturated iron is considered to be given by last point of its B-H curve as

$$\mu_{sat} = \frac{B_{last}}{H_{last}} \quad . \tag{1}$$

- The magnetic flux lines leave and enter the permanent magnet on the top and the bottom of the permanent magnet only.
- The magnetic flux density on a single leakage path is constant.

B. Analytical Model of the Magnetic Circuit

A permanent magnet placed in such an environment generates magnetomotive force, whose reaction is generation of magnetic flux. The main part of the magnetic flux goes through the air gap to the stator (main magnetic flux Φ_δ) and a part of the magnetic flux forms a loop on sides of the permanent magnets while another part goes through the air gap to the opposite rotor pole. Both these parts form the leakage magnetic flux Φ_σ.

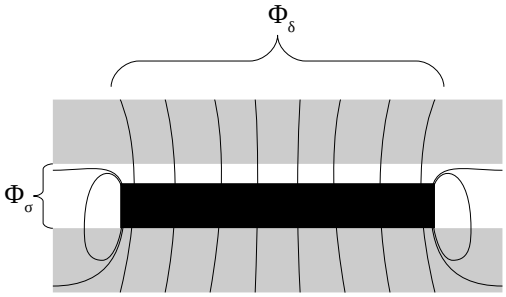

Fig. 2. Schematic visualization of permanent magnet magnetic flux, its leakage through the air gap and on sides of the permanent magnet.

The paths of the magnetic flux lines shown in Fig. 2 may be then substituted by a reluctance network shown in Fig. 3. Considering machine symmetry, the whole network which repeats in general $2p$ times may be divided by symmetry axes, i.e. q-axes of the machine.

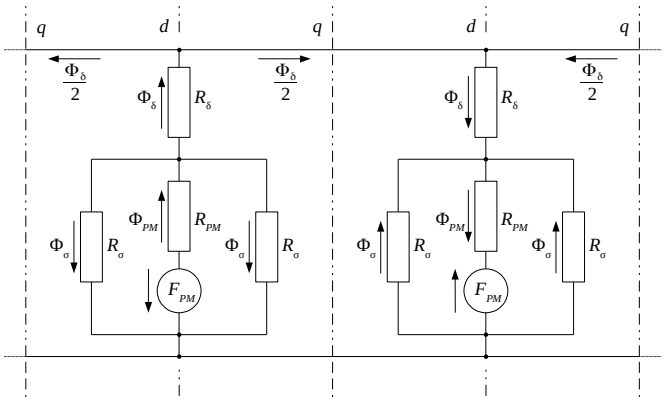

Fig. 3. Parts of the general reluctance network.

Among the magnetomotive force of the permanent magnet F_{PM} generating the magnetic field, it includes its own (inner) magnetic reluctance R_{PM}, reluctance of the air gap R_δ and the reluctance of the leakage paths R_σ. According to equivalent circuit shown in Fig. 3, the magnetomotive force drops equality on the air gap and leakage paths is given by magnetic field strengths and flux lines lengths as

$$\Delta F = \oint_{\delta'} H_\delta dl = \oint_{l_{\sigma i}} H_{\sigma i} dl \quad , \tag{2}$$

whereas the magnetic flux through the air gap is known from air gap magnetic flux density and machine dimensions [12]

$$\Phi_\delta = \oint_{S_\delta} B_\delta(\xi) dS = \alpha_\delta B_\delta t_p l \quad . \tag{3}$$

Since the air gap is magnetically linear environment, the air gap magnetic field strength may be derived from the air gap magnetic flux density using air permeability as

$$B_\delta = \mu_0 H_\delta \quad . \tag{4}$$

C. Permanent Magnet Leakage Flux Factor

To be able to compare previously mentioned rotor topologies, it is suitable to introduce the leakage of magnetic flux as a single dimensionless factor. To be consistent with general theory of synchronous machines [12] it is possible to modify the field winding leakage factor to permanent magnet leakage flux factor defined by a ratio of permanent magnet and air gap magnetic fluxes as

$$k_\sigma = \frac{\Phi_{PM}}{\Phi_\delta} \quad , \tag{5}$$

where the total permanent magnet magnetic flux results from the node in the equivalent circuit in Fig. 3

$$\Phi_{PM} + 2\Phi_\sigma + \Phi_\delta = 0 \quad . \tag{6}$$

IV. Permanent Magnet Leakage Flux Factors of Different Rotor Layouts

A. Permanent Magnets Placed on the Surface of the Rotor

A schematic drawing of surface mounted permanent magnet and its leakage fluxes is shown in Fig. 4. Among the main magnetic flux path through the air gap one of the leakage fluxes goes through the air gap to neighbouring magnet on opposite pole (denoted as σ_1) and a part of the magnetic flux encloses around the side of the permanent magnet (denoted as σ_2). Presuming mechanical permanent magnet pole coverage factor α_{PM} and machine pole pitch t_p, the length of the magnetic flux line between neighbouring magnets is

$$l_{\sigma 1} = (1-\alpha_{PM})\frac{t_p}{2} \quad . \tag{7}$$

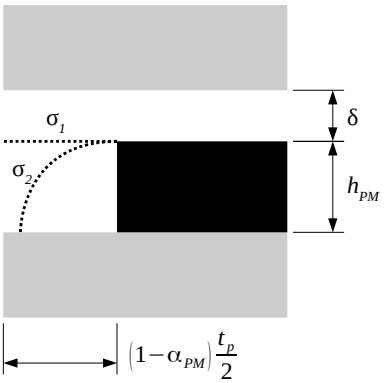

Fig. 4. Surface mounted permanent magnet leakage paths.

The length of the magnetic flux line from the top of the magnet to the rotor surface may be approximated by a quarter of a circle with radius equal to permanent magnet height h_{PM}, thus its length is

$$l_{\sigma 2} = \frac{1}{2}\pi h_{PM} \quad , \tag{8}$$

The leakage magnetic flux σ_1 uses the whole air gap length in both radial and axial directions, hence its total magnetic flux is

$$\Phi_{\sigma 1} = \int_{S_{\sigma 1}} B_{\sigma 1} dS = \int_l \int_\delta B_{\sigma 1} dy\, dz = B_{\sigma 1} \delta l \quad , \tag{9}$$

whereas the magnetic flux density on this leakage path results from equality of magnetomotive force drops on the air gap and the leakage path as defined by (2), in this case

$$H_\delta \delta' = H_{\sigma 1} l_{\sigma 1} \quad , \tag{10}$$

which gives

$$B_{\sigma 1} = \mu_0 H_{\sigma 1} = \mu_0 H_\delta \frac{\delta'}{(1-\alpha_{PM})\frac{t_p}{2}} \quad , \tag{11}$$

where the electromagnetic air gap length δ' is its mechanical length multiplied by Carter's factor k_C:

$$\delta' = k_C \delta \quad . \tag{12}$$

In case of surface mounted permanent magnets (both "S" and "B" topologies) the air gap of the machine is increased by the thickness of permanent magnets (their material relative permeability μ_{rPM} is close to the air), so the Carter's factor is calculated from slot pitch t_s and slot opening width b_o as in [13]

$$k_C = \frac{t_s}{t_s - \gamma b_o} \tag{13}$$

whereas the γ factor includes both mechanical air gap length δ and permanent magnet thickness modified by permanent magnet permeability μ_{rPM}

$$\gamma = \frac{b_o}{b_o + 5\left(\delta + \frac{h_{PM}}{\mu_{rPM}}\right)} \quad . \tag{14}$$

In case of the leakage magnetic flux σ_2 it does not leave the permanent magnet only on its top, but also on its sides. Presuming homogeneous magnetic flux density on whole cross-section of the leakage path σ_2, the total magnetic flux of this leakage path results

$$\Phi_{\sigma 2} = \int_{S_{\sigma 2}} B_{\sigma 2} dS = \int_l \int_{\frac{h_{PM}}{2}} B_{\sigma 2} dy\, dz = B_{\sigma 2} \frac{h_{PM}}{2} l \quad , \tag{15}$$

where the magnetic flux density on this leakage path may be derived as an alternative to magnetic flux density $B_{\sigma 1}$ using

$$B_{\sigma 2}=\mu_0 H_{\sigma 2}=\mu_0 H_\delta \frac{\delta'}{\pi\frac{h_{PM}}{2}} \quad . \tag{16}$$

For geometric layout shown in Fig. 4 the magnetic flux leakage factor results according to (5)

$$k_\sigma=\frac{\Phi_\delta+2\left(\Phi_{\sigma 1}+\Phi_{\sigma 2}\right)}{\Phi_\delta} \quad , \tag{17}$$

and after substitution and modification it gives

$$k_\sigma=1+2\left[\frac{2k_C\delta^2}{\alpha_\delta\left(1-\alpha_{PM}\right)t_p^2}+\frac{k_C\delta}{\pi\alpha_\delta t_p}\right] \quad . \tag{18}$$

B. Bread-shaped Permanent Magnets on the Rotor Surface

By introduction of the permanent magnet curvature, its sides shorten and a wider gap is opened for the leakage magnetic flux to go between machine poles (see Fig. 5). The relation between mechanical air gap δ and air gap on the edges of the permanent magnet δ_{max} can be introduced as air gap factor

$$k_\delta=\frac{\delta_{max}}{\delta} \quad . \tag{19}$$

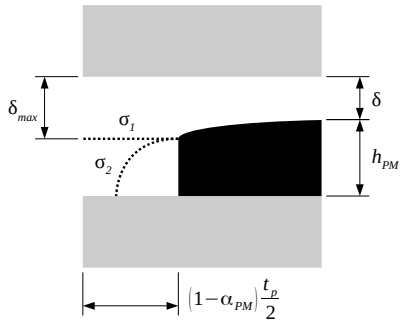

Fig. 5. Bread-shaped surface mounted permanent magnet leakage paths.

Using similar approach as in section IV-A, it is necessary to modify the magnetic flux through the leakage path σ_1 to

$$\Phi_{\sigma 1}=B_{\sigma 1}k_\delta\delta l \quad . \tag{20}$$

The radius of the leakage path σ_2 further reduces from central permanent magnet height h_{PM} to

$$r_{\sigma 2}=h_{PM}-\left(k_\delta-1\right)\delta \tag{21}$$

and equivalently to (15) the magnetic flux through leakage path σ_2 results

$$\Phi_{\sigma 2}=B_{\sigma 2}\frac{r_{\sigma 2}}{2}l=B_{\sigma 2}\frac{h_{PM}-\left(k_\delta-1\right)\delta}{2}l \quad . \tag{22}$$

The magnetic flux density in the volume of the leakage path σ_2 is then

$$B_{\sigma 2}=\mu_0 H_{\sigma 2}=\mu_0 H_\delta \frac{\delta'}{\pi\frac{r_{\sigma 2}}{2}}= =\mu_0 H_\delta \frac{\delta'}{\pi\frac{h_{PM}-\left(k_\delta-1\right)\delta}{2}} \quad . \tag{23}$$

The permanent magnet leakage flux factor for bread shaped permanent magnets mounted on the surface of the rotor then results

$$k_\sigma=1+2\left[\frac{2k_\delta k_C\delta^2}{\alpha_\delta\left(1-\alpha_{PM}\right)t_p^2}+\frac{k_C\delta}{\pi\alpha_\delta t_p}\right] \quad , \tag{24}$$

whereas from comparison with result (18) it is obvious, that (24) is a generalization of the relation for rectangular permanent magnets placed on the rotor surface. From the physical principle it is also evident, that identical relation will be valid for rectangular permanent magnets equipped with ferromagnetic pole-shoes, but in this case the γ factor for calculation of Carter's factor must be derived from mechanical air gap length only in the same way as in case of interior permanent magnets as noted below in (29).

C. Tangential Interior Permanent Magnets

In case of tangentially placed interior permanent magnets they are located in a ferromagnetic material, which significantly increases the leakage magnetic flux of the permanent magnets (see Fig. 6). To avoid excessive increase of the leakage magnetic flux, the permanent magnets are placed possibly closest to the air gap and the bridges between neighbouring poles are designed to be possibly thinnest which is further limited by mechanical constraints.

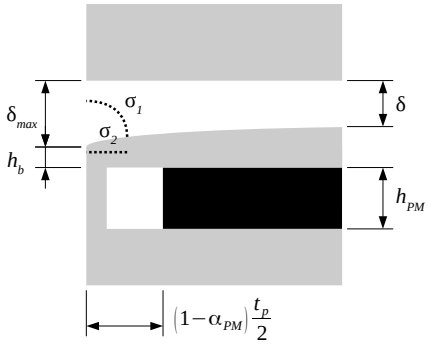

Fig. 6. Leakage paths of tangentially placed permanent magnets.

In comparison to previously analysed permanent magnet placements the main part of the leakage magnetic flux is led through (saturated) bridges between neighbouring poles (denoted as σ_2) and only a part of the leakage magnetic flux is led through parallel path in the air gap (denoted as σ_1). An additional part of the leakage magnetic flux is also present in the gap on sides of the permanent magnet, but due to hard

description of its shape it will be neglected in further calculation.

Presuming that the magnetic flux lines of both leakage paths origin in one half of the length of the bridge between the permanent magnet and the *q* axis of the rotor, the length of the leakage path σ_2 and the radius of the leakage path σ_1 are identical and they are

$$l_{\sigma 2}=r_{\sigma 1}=\frac{1}{2}\left(1-\alpha_{PM}\right)\frac{t_p}{2} \quad . \tag{25}$$

Presuming the leakage path σ_1 is a quarter of a circle, its length is

$$l_{\sigma 1}=\pi\frac{r_{\sigma 1}}{2}=\pi\left(1-\alpha_{PM}\right)\frac{t_p}{8} \quad . \tag{26}$$

Similarly to previous sections, the magnetic field strength on leakage path σ_1 results

$$H_{\sigma 1}=H_\delta\frac{\delta'}{l_{\sigma 1}}=H_\delta\frac{8\delta'}{\pi\left(1-\alpha_{PM}\right)t_p} \tag{27}$$

and, presuming that the magnetic flux utilizes the whole air gap length, the magnetic flux through leakage path σ_1 is

$$\Phi_{\sigma 1}=\mu_0 H_\delta\frac{8k_\delta k_C\delta^2 l}{\pi\left(1-\alpha_{PM}\right)t_p} \quad , \tag{28}$$

whereas in case of interior permanent magnets (topologies "V", "T" and "P") the curvature of magnetic flux lines in the air gap corresponds to standard electric machines, thus the γ factor for calculation of the Carter's factor is obtained as

$$\gamma=\frac{b_o}{b_o+5\delta} \quad . \tag{29}$$

The magnetic field strength on leakage path σ_2 results from equality of magnetomotive force drops on all magnetic flux paths as

$$H_{\sigma 2}=H_\delta\frac{\delta'}{l_{\sigma 2}} \quad , \tag{30}$$

but since this path leads through saturated steel bridge between the poles, the magnetic flux density in the bridge with height h_b results

$$B_{\sigma 2}=\mu_{sat}H_{\sigma 2} \quad . \tag{31}$$

The magnetic flux through leakage path σ_2 is then

$$\Phi_{\sigma 2}=\mu_{sat}H_\delta\frac{k_C\delta h_b l}{l_{\sigma 2}} \quad . \tag{32}$$

The permanent magnet leakage flux factor for tangentially placed interior permanent magnets results

$$k_\sigma=1+2\left[\frac{8k_\delta k_C\delta^2}{\alpha_\delta\pi\left(1-\alpha_{PM}\right)t_p^2}+\mu_{rsat}\frac{4k_C\delta h_b}{\alpha_\delta\left(1-\alpha_{PM}\right)t_p^2}\right] \quad , \tag{33}$$

where μ_{rsat} is the relative permeability of saturated steel derived from μ_{sat}.

D. V-shaped Interior Permanent Magnets

The V-shaped interior permanent magnets have very similar magnetic properties as the tangentially placed permanent magnets, but as an addition a central bridge in the *d*-axis is present (see Fig. 7). Since this bridge is located directly between permanent magnets, is is saturated in its whole length.

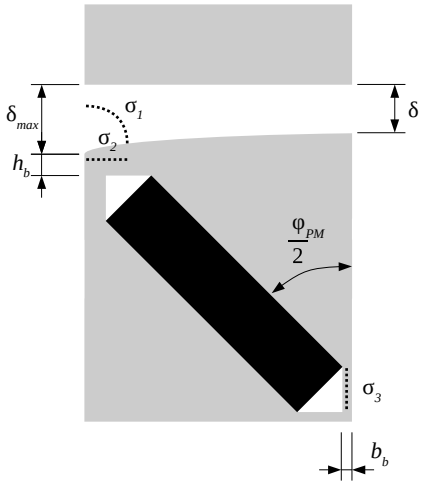

Fig. 7. Leakage paths of V-shaped interior permanent magnets.

Hence, to obtain the permanent magnet leakage flux factor of V-shaped interior permanent magnets it is possible to to use relations derived for tangential interior permanent magnets with third leakage magnetic flux added. Since the permanent magnets are beveled from each other under angle φ_{PM}, the length of leakage path σ_2 and the radius of leakage path σ_1 reduces to

$$l_{\sigma 2}=r_{\sigma 1}=\frac{h_{PM}}{2}\cos\frac{\varphi_{PM}}{2}+b_b \quad , \tag{34}$$

and in presumed geometry the length of leakage path σ_3 is

$$l_{\sigma 3}=h_{PM}\sin\frac{\varphi_{PM}}{2} \quad . \tag{35}$$

The leakage magnetic flux along path σ_3 then results

$$\Phi_{\sigma 3}=\mu_{sat}H_\delta\frac{k_C\delta b_b l}{h_{PM}\sin\frac{\varphi_{PM}}{2}} \tag{36}$$

and the leakage magnetic flux factor for V-shaped interior permanent magnets is then

$$k_\sigma = 1 + 2\left[\frac{2k_\delta k_C \delta^2}{\alpha_\delta t_p \pi\left(\frac{h_{PM}}{2}\cos\frac{\varphi_{PM}}{2} + b_b\right)} + \right.$$
$$\left. + \mu_{rsat}\frac{k_C \delta h_b}{\alpha_\delta t_p\left(\frac{h_{PM}}{2}\cos\frac{\varphi_{PM}}{2} + b_b\right)} + \mu_{rsat}\frac{k_C \delta b_b}{\alpha_\delta h_{PM}\sin\frac{\varphi_{PM}}{2} t_p}\right] \quad .(37)$$

V. Verification of Results using Finite Element Method

The verification of analytically obtained results was performed using open-source software FEMM [14] as a magnetostatic task. The machine used for the purpose of the study was a prototype of a 10 pole traction permanent magnet synchronous machine with 45 stator slots and rated power of 150 *kW*, whereas the main aim of the comparative design was keeping possibly closest total permanent magnet volume. Due to limited symmetry of the machine its whole geometry was modelled.

The material properties of used materials are shown in Tables I and II, whereas the material properties of the permanent magnets are based on minimal data sheet parameters provided by the manufacturer [15] while the parameters of the electrical steel are manufacturer's own measured parameters from delivered samples.

TABLE I
Material Properties of Used Permanent Magnets

material	N35UH
B_r [*T*]	1.17
H_c [*A/m*]	860000
μ_{rPM} [*H/m*]	1.08

TABLE II
Material Properties of Used Lamination
(Selection of Most Significant points)

material	M330-50A			
B [*T*]	1.5	1.6	1.7	2.65
H [*A/m*]	5590	8600	12500	311874

The permanent magnet leakage flux factor was derived from magnetic flux going from the rotor to the stator over one pole pitch as

$$\Phi_\delta = \oint_S B_\delta(\xi)\, dS \quad , \qquad (38)$$

where the values of air gap magnetic flux density B_δ were read on a line drawn on inner surface of the stator. The total magnetic flux generated by permanent magnets was then derived from maxima and minima of the magnetic vector potential in the whole task [16] as

$$\Phi_{PM} = (A_{max} - A_{min})\, l \quad , \qquad (39)$$

where l is the task depth ($l = 0.286\ m$).

The permanent magnet leakage flux factor is then calculated using (5). The summary of obtained results is listed in Table III, the magnetic flux lines obtained from the simulations are shown in Fig. 8.

TABLE III
Results Obtained using Finite Element Method

	magnet layout				
	S	B	V	T	P
Φ_δ [*mWb*]	18.18	16.63	15.46	17.06	19.62
A_{max} [*Wb/m*]	0.032486	0.029846	0.034475	0.037766	0.035185
A_{min} [*Wb/m*]	-0.032505	-0.029825	-0.034467	-0.037745	-0.035187
Φ_{PM} [*mWb*]	18.59	17.07	19.72	15.46	20.13
k_σ [-]	1.022	1.026	1.275	1.266	1.026

The analytically calculated results according to relations (18), (24), (33) and (37) and their comparison with results from the finite element method analysis are shown in Table IV. The percentual difference between the results was calculated as

$$\delta k_\sigma = \frac{k_\sigma - k_{\sigma FEM}}{k_{\sigma FEM}} \cdot 100 \quad . \qquad (40)$$

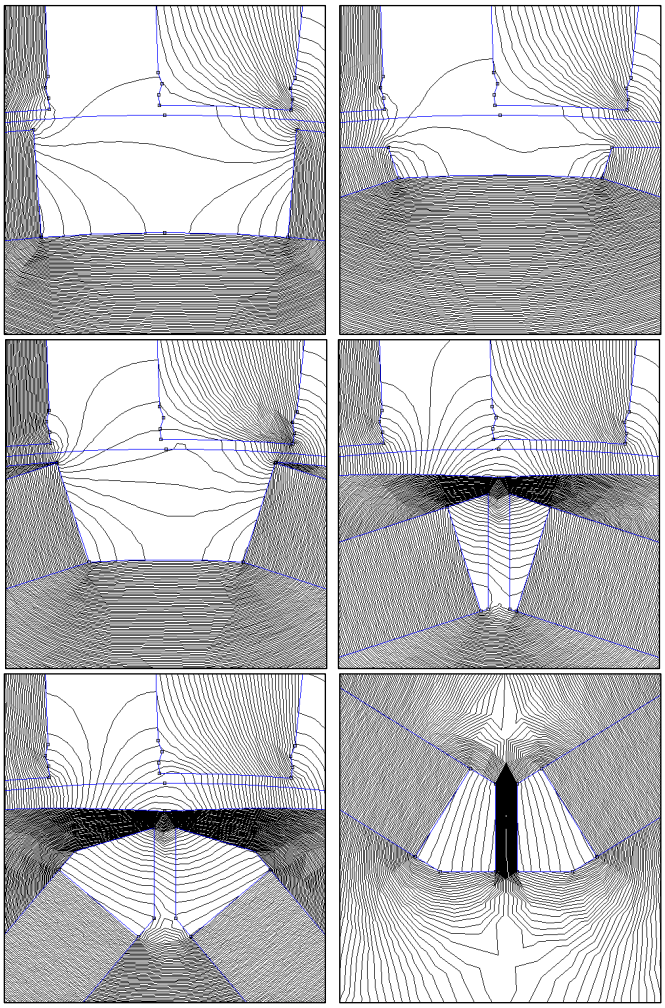

Fig. 8. Details of magnetic flux lines of leakage magnetic fluxes in layouts "S", "B", "P", "T" and "V" (left-to-right).

TABLE IV
COMPARISON OF RESULTS OF ANALYTICAL CALCULATION WITH FEM

layout	k_σ [-]	$k_{\sigma FEM}$ [-]	δk_σ [%]
S	1.028	1.022	0.59
B	1.037	1.026	1.04
V	1.264	1.275	-0.92
T	1.210	1.266	-4.39
P	1.031	1.026	0.57

VI. CONCLUSION

Although the presented analytical approach to calculation of permanent magnet leakage fluxes uses many simplifying conditions, the results of analytical calculations correspond with finite element method analyses in order of per cent. When comparing the obtained results with results derived in other literature they correspond also with results obtained using different approaches. This means that derived relations may be successfully used for design of permanent magnets in most common rotor topologies, while the simplicity of obtained solution allows fast calculation of the permanent magnet leakage factor and implementation of such a calculation into a higher algorithm.

The comparison of results between different rotor layouts show, that lowest leakage magnetic flux appears when permanent magnets are not placed in ferromagnetic environment, which corresponds to surface mounted permanent magnets. The placement of permanent magnets into ferromagnetic environment (interior permanent magnets) increases the permanent magnet leakage flux, so it may reach up to 25 per cent of the air gap magnetic flux.

As a result the interior permanent magnet layouts are least advantageous from material consumption point of view since they require approximately 25 per cent higher mass of permanent magnets to achieve identical air gap magnetic flux as the surface mounted permanent magnets. As a counter point another advantages of interior permanent magnets have to be considered – lower effect of air gap harmonic components regarding permanent magnet losses and higher saliency resulting in additional reluctance torque of interior permanent magnet machine.

VII. REFERENCES

[1] J. S. Yoo et al., "Design of Rotor with Novel Barrier for Power Improvement of Spoke-Type Permanent Magnet Synchronous Motor," *2018 21st International Conference on Electrical Machines and Systems* (ICEMS), 2018, pp. 252-255, doi: 10.23919/ICEMS.2018.8549221.

[2] Z. Chen, H. Ma and Z. Li, "Rotor parameter analysis for surface-mounted and interior hybrid permanent magnet synchronous machine," *2016 19th International Conference on Electrical Machines and Systems* (ICEMS), 2016, pp. 1-5.

[3] Chang-Chou Hwang and Y. H. Cho, "Effects of leakage flux on magnetic fields of interior permanent magnet synchronous motors," in *IEEE Transactions on Magnetics*, vol. 37, no. 4, pp. 3021-3024, July 2001, doi: 10.1109/20.947055.

[4] A. Daghigh, H. Javadi and A. Javadi, "Improved Analytical Modeling of Permanent Magnet Leakage Flux in Design of the Coreless Axial Flux Permanent Magnet Generatorx," in *Canadian Journal of Electrical and Computer Engineering*, vol. 40, no. 1, pp. 3-11, winter 2017, doi: 10.1109/CJECE.2016.2550667.

[5] G. M. Kiss and I. Vajda, "Magnet leakage flux of axial flux PM synchronous machines for EV," *2014 IEEE International Electric Vehicle Conference* (IEVC), 2014, pp. 1-5, doi: 10.1109/IEVC.2014.7056206.

[6] K. Guo, Y. Guo and S. Fang, "Flux Leakage Analytical Calculation in the E-shape Stator of Linear Rotary Motor with Interlaced Permanent Magnet Poles," in *IEEE Transactions on Magnetics*, doi: 10.1109/TMAG.2022.3147448.

[7] K. Lu, P. O. Rasmussen and E. Ritchie, "Design Considerations of Permanent Magnet Transverse Flux Machines," in *IEEE Transactions on Magnetics*, vol. 47, no. 10, pp. 2804-2807, Oct. 2011, doi: 10.1109/TMAG.2011.2146758.

[8] S. G. Lee, J. Bae and W. Kim, "Study on the Axial Leakage Magnetic Flux in a Spoke Type Permanent Magnet Synchronous Motor," in *IEEE Transactions on Industry Applications,* vol. 55, no. 6, pp. 5881-5887, Nov.-Dec. 2019, doi: 10.1109/TIA.2019.2939743.

[9] Zhao Xiaobo and Ji Changying, "Analysis of flux leakage in novel permanent magnet type eddy current retarder for vehicle applications," 2008 *IEEE Vehicle Power and Propulsion Conference*, 2008, pp. 1-4, doi: 10.1109/VPPC.2008.4677735.

[10] N. Saed, S. Asgari and M. Mirsalim, "Zigzag leakage flux modeling in permanent magnet machines with cylindrical magnets, "*2018 9th Annual Power Electronics, Drives Systems and Technologies Conference* (PEDSTC), 2018, pp. 95-98, doi: 10.1109/PEDSTC.2018.8343778.

[11] W. Wu, Y. Sun, Y. Wu, S. Zong and W. Wu, "Design and Analysis of Adjustable Flux Leakage Characteristics in IPM Synchronous Machine Based on Regression Orthogonal Method," *2020 IEEE International Conference on Applied Superconductivity and Electromagnetic Devices* (ASEMD), 2020, pp. 1-2, doi: 10.1109/ASEMD49065.2020.9276070.

[12] J. Pyrhönen, T. Jokinen and V. Hrabovcova, *Design of Rotating Electrical Machines*. John Wiley & Sons, Chichester, UK, 2014. ISBN 978-1-118-58157-5

[13] G. Müller, K. Vogt, B. Ponick, *Calculations of Electric Machines* (*Berechnung Elektrischer Maschinen*). WILEY Verlag, Weinheim, Germany, 2007. ISBN 9783-5274-0525-1

[14] Meeker, D. C.: *Finite Element Method Magnetics, Version 4.2 (28Feb2018 Build)*, http://www.femm.info

[15] Arnold Magnetic Technologies Corp.: *N35UH - Sintered Neodymium-Iron-Boron Magnets*, https://www.arnoldmagnetics.com/wp-content/ /uploads/2017/11/N35UH-151021.pdf

[16] Bianchi, N., *Electrical Machine Analysis Using Finite Elements*. CRC Press, Boca Raton, USA, 2005. ISBN 978-0-849-33399-6

VIII. BIOGRAPHIES

K. Hruska (M'20) was born in Ostrov in the Czechoslovak Socialist Republic on January 16, 1983. He graduated from the University of West Bohemia in 2007.

Since 2018 he is a reader at the Faculty of Electrical Engineering, University of West Bohemia. He lectures courses of electric machines, theory of electric machines and design of electric machines. As a member of Research and Innovation Centre for Electrical Engineering he leads the Electric Machines Group and he is active in research and development related to electric machines.

P. Dvorak (M'16) was born in Litomerice in the Czechoslovak Socialist Republic on April 29, 1978. He graduated from the University of West Bohemia in 2003.

Since 2005 he is employed in SKODA ELECTRIC a.s. Since 2014 he works as a researcher in Research and Development Department of the SKODA ELECTRIC and his activity is focused on research of the traction motors based on asynchronous motors and synchronous motors with permanent magnets for wheel propulsion of public transport vehicles.